ISSN : 0974 - 7486 Volume 10 Issue 7

Materials Science

An Indian Journal

Full Paper

MSAIJ, 10(7), 2014 [247-256]

Thermodynamic study, elaboration and high temperature oxidation of alloys highly strengthened by tantalum carbides. Part 3: Case of a Fe-30Cr-1C-15Ta alloy

Laura Corona[1,2], Patrice Berthod[1,2,3]*

[1]University of Lorraine, B.P. 70239, 54506 Vandoeuvre-lès-Nancy, (FRANCE)

[2]Faculty of Sciences and Technologies, B.P. 70239, 54506 Vandoeuvre-lès-Nancy, (FRANCE)

[3]Institut Jean Lamour (UMR 7198), Team 206 "Surface and Interface, Chemical Reactivity of Materials", B.P. 70239, 54506 Vandoeuvre-lès-Nancy, (FRANCE)

E-mail : Patrice.Berthod@univ-lorraine.fr

ABSTRACT

This third part of the present work about chromium-rich alloys containing high amounts in carbon and tantalum, concerns a Fe-30Cr-1C-15Ta alloy. Its elaboration by high frequency induction foundry, here too after preliminary thermodynamic calculations, led to an alloy impoverished in tantalum by comparison with the targeted content and presenting a microstructure different from the one which was expected. The tantalum carbides were neither the single carbide phase nor present with volume fractions high enough to ensure high hardness. Finally, the alloy obtained, characterized by chromium and tantalum contents of 34 wt.% and 5.7 wt.% respectively, showed a microstructure with a dendritic matrix and numerous eutectic chromium carbides and tantalum carbides potentially useful for creep-resistance at high temperature. If its moderate hardness does not permit envisaging wear applications, the very good resistance to hot oxidation showed by the obtained alloy may be of interest for high temperature applications in aggressive gases.

KEYWORDS

Iron alloys;
Tantalum carbides;
Thermodynamic calculations;
Microstructures;
Hardness;
High temperature oxidation.

INTRODUCTION

The alloys based on iron and containing also carbon have often a rather high hardness, which can vary over a rather wide range because of the presence of hard phases or compounds obtained by fast solidification[1] or by quenching in solid state from the austenitic temperature range[2]. These ones can be the iron carbide Fe_3C cementite, the eutectoid compound {ferrite + cementite} named pearlite, or the unstable phase martensite. Such hard particles or compounds can be found first in simple binary Fe-C alloys but also in more complex iron-based alloys, for instance those containing also chromium (which belongs to the carbide-forming and carbide-stabilizer elements) especially added to enhance the hardness of bulk iron-based materials[3] as well as coatings[4]. The presence of such phases or compounds induce great values of hardness, results which can be

wished (for favouring wear resistance for example) or not (for preserving ductility). The same phases also favouring brittleness it is often necessary to control if such phases are present or not in the microstructure, what can be simply done by hardness measurement[5].

Very high fractions of chromium carbides can be obtained in iron-based alloys to achieve especially high levels of hardness[6-7], by adding a lot of carbon in presence of sufficiently high chromium content. Such high carbon content, which can reach values more commonly met in cast irons (near 4 or 5wt.%C), may be detrimental for the refractoriness of the alloys (if such property is required for the considered application). As for the chromium-rich cobalt-based[8] and nickel-based[9] alloys of the first part and second part of this work, another carbide-former element (stronger than chromium) was considered – tantalum – in order to develop a dense network of hard carbides without increasing too much the carbon content (by limiting it at 1wt.%C) and to maintain the solidus temperature at a high level. The contents in carbon and tantalum which were targeted here are the same as for the two former alloys (1wt.% and 15wt.% respectively), and the alloy was elaborated following the same route (melting in an High Frequency induction furnace, rather fast cooling and solidification). The as-cast microstructure and the level of hardness of the obtained alloy, as well as its behaviour in oxidation at high temperature, were studied, again in order to judge its potential as representing a possible alternative to alloys hardened with other carbides.

EXPERIMENTAL

Similarly to what was done for the cobalt alloy and the nickel one, subjects of the first part and of the second one of this study, the work was started by performing thermodynamic calculations to describe the microstructure development during solidification and solid state cooling. For that, the Thermo-Calc version N software[10] was used again. The used database (SSOL[11]) initially contained the descriptions of the Fe-C[12], Fe-Cr[13], C-Cr[14] and Fe-C-Cr[15]. For allowing calculations in the quaternary system Fe-Cr-C-Ta, the descriptions of supplementary systems (as Ta-C[16] or Ta-Cr[17]) were added. The theoretic appearance and disappearance of the successive phases in the liquid and solid Fe-30Cr-1C-15Ta (wt.%) alloy were determined using this thermodynamic calculation tool, as well as their theoretic mass fractions and chemical compositions versus temperature (again from the solidification start temperature down to 500°C).

The real alloy was also synthesized by foundry from pure elements (Fe, Cr and Ta: Alfa Aesar, purity higher than 99.9 wt.%; C: graphite), under 300mbars of pure Argon. The initial melting of the pure elements together was achieved using the CELES high frequency induction furnace, while solidification occurred in its water–cooled copper crucible. The obtained 40g-weighing ingot was cut to obtain two parts, one for the as-cast microstructure observations and the 30kg-Vickers hardness measurements (Testwell Wolpert), and one for the exposure to 1150°C for 46h in air for specifying the alloy's behavior in high temperature oxidation. The latter operation was realized in a resistive tubular furnace with the second sample after preliminary polishing with 1200-grade SiC paper. The applied thermal cycle started by a heating at +20°C min^{-1} up to 1150°C (stage temperature) at which it was maintained during 46 hours, and finished by a slow cooling in the shut-off furnace.

The two samples, the as-cast one and the oxidized one (preliminarily covered by electrolytic Ni-coating to mechanically protect the oxide scale), were cut and embedded in a cold resin mixture (resin CY230 + hardener HY956). Polishing was done with SiC papers from 240 to 1200 grit, then with a textile disk enriched with 1µm alumina particles. Microstructure and oxides were observed in cross-section using a Scanning Electron Microscopy (SEM JEOL JSM-6010LA), mainly in Back Scattered Electrons mode (BSE) under an acceleration voltage of 20kV. The chemical composition determination was realized by using the Energy Dispersion Spectrometry (EDS) apparatus equipping the SEM.

RESULTS AND DISCUSSION

Thermodynamic calculations

The theoretic evolution of the metallurgical state of the Fe-30Cr-1C-15Ta (wt.%) alloy was obtained by performing Thermo-Calc calculations for successive temperatures from 2000 to 500°C, every 50 or 100°C depending on what happened in the considered tem-

perature range, to know each time the present phases as well as their mass fractions. This led to the graphs presented in Figure 1, the first one (A) for all the phases together, and the second one (B) for the phases with the lowest mass fractions (carbides) by vertical enlargement of the first graph. It appears that the first solid phase to appear when the liquid temperature has decreased to 2000°C is the TaC carbide one. Theoretically this phase is the single solid one to exist during the cooling over almost 500°C, before the second solid phase to appear – the matrix – starts crystallizing. This one, which is of the Back Centred Cubic form, entirely solidifies over about 100°C (i.e. much less than the TaC phase), partly in eutectic with the TaC carbides the mass fraction of which keeps on increasing until reaching the solidus temperature. The mass fractions of the only two present solid phases (BCC matrix + TaC carbide) would not evolve over the about 700 following °C of cooling. When temperature reaches about 800°C a significant part of matrix (about half of it) seemingly should transform into sigma phase and traces of chromium carbides ($Cr_{23}C_6$) would appear simultaneously. Finally, according to Thermo-Calc calculations, the microstructure of the alloy should be composed of 46.34mass.% of Sigma phase, 37.57 mass.% of BCC matrix, 16mass.% of TaC carbides and only 0.1mass.% of $Cr_{23}C_6$ chromium carbides.

The variation of mass fraction of liquid phase is plot-

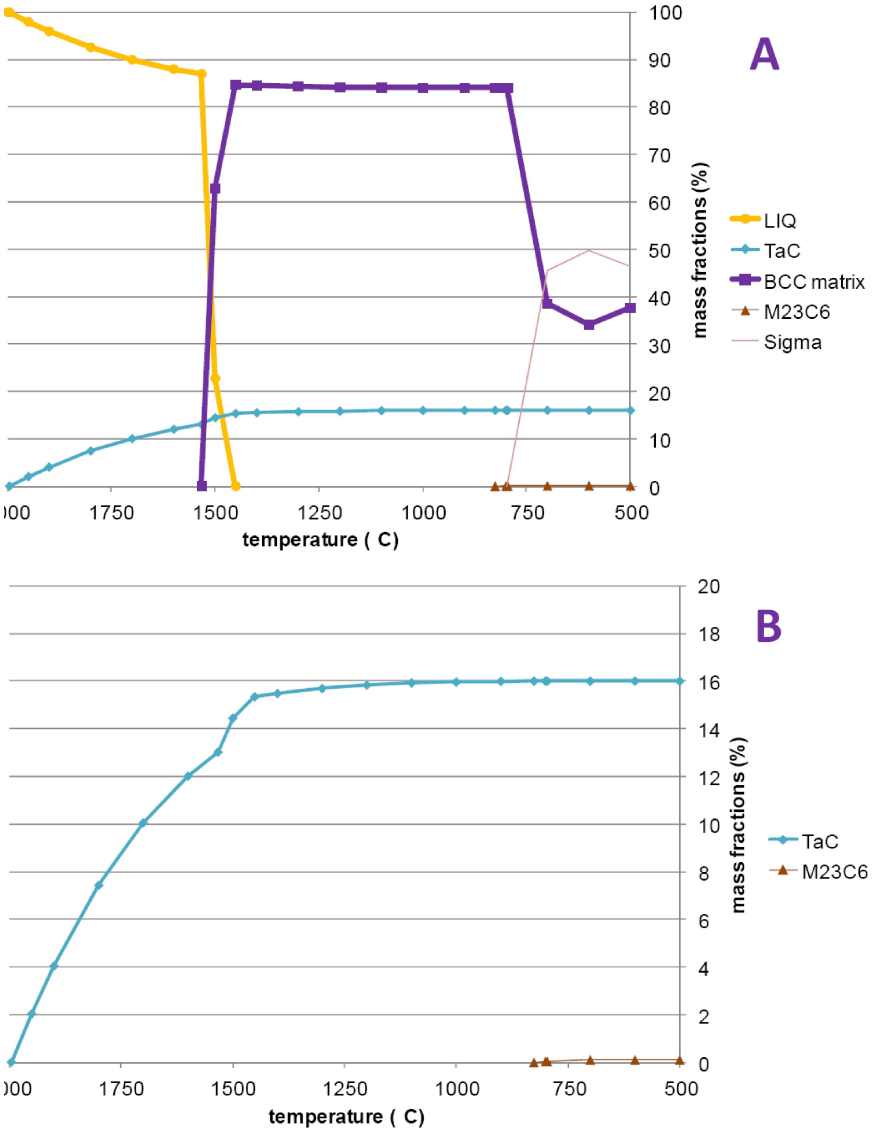

Figure 1 : Development of the microstructure of the Fe-30Cr-1C-15Ta alloy during solidification, according to Thermo-Calc (B : enlargement of the low mass fractions part of A)

ted again in Figure 2 but with an abscissa (temperature) increasing axis, together with the contents of this liquid phase in the different elements versus temperature. The liquid chemical composition should evolve during solidification from 30Fe-15Ta-1C (bal. Fe: 54) (wt.%) at the liquidus temperature (which is of about 2000°C) to 36.71Cr-1.07Ta-0.85C (bal. Fe: 61.38) (wt.%). Thus a chromium positive segregation can be expected, with as result a chromium enrichment in the last solidified zones.

The chemical composition of the TaC phase versus temperature is plotted in Figure 3. According to Thermo-Calc, TaC is not exactly a stoichiometric carbide since its composition slightly change with temperature. This is the most visible by considering its weight carbon content which increases from 5.36 2000°C (1995.64°C) to 6.22 at 500°C. The Ta content (major element) and the Cr and Fe contents (traces) do not present so noticeable variations.

The chemical composition variation of the BCC phase with temperature is graphically represented in Figure 4. During solidification the chemical composi-

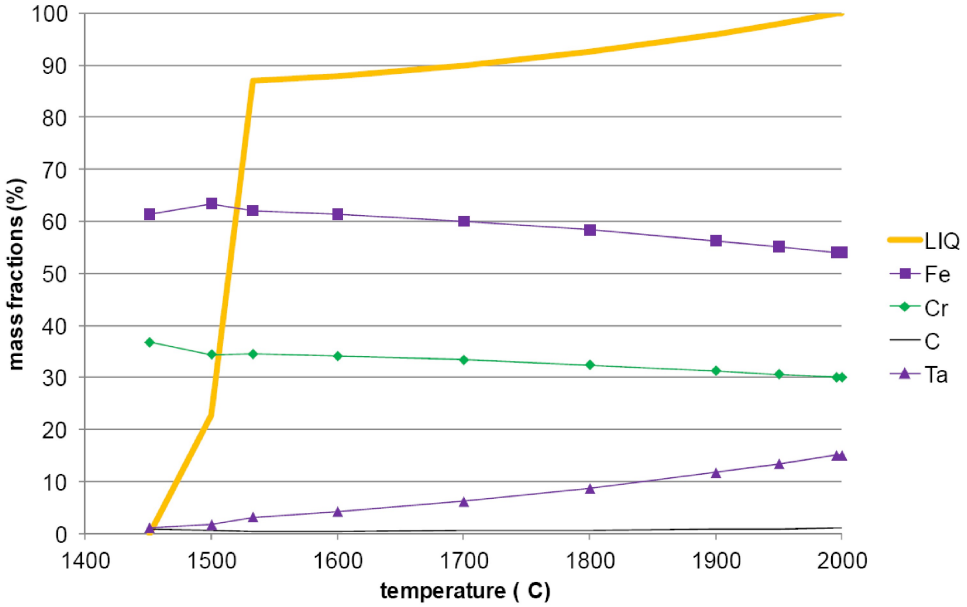

Figure 2 : Evolution of the chemical composition of the liquid phase with temperature (according to Thermo-Calc)

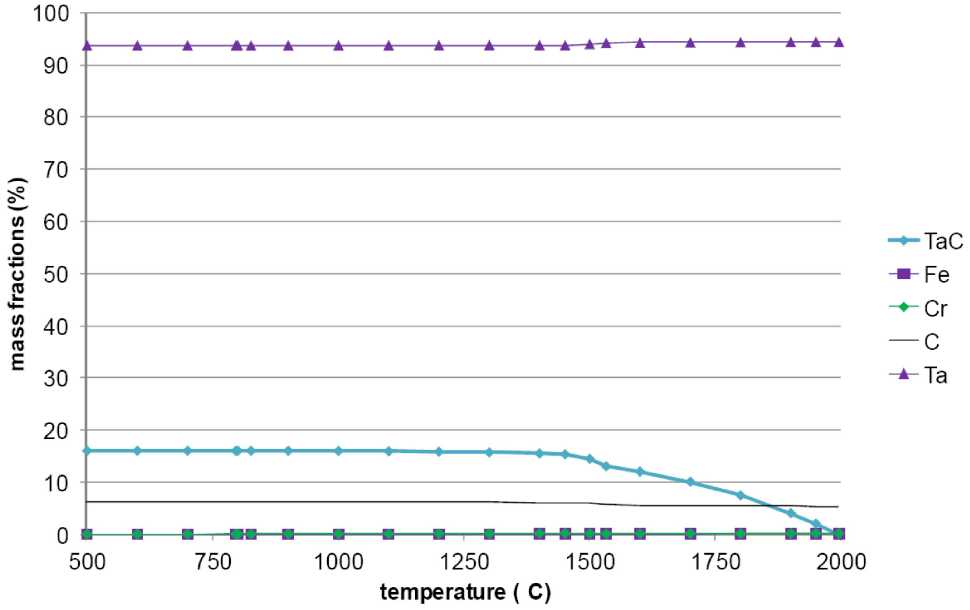

Figure 3 : Evolution of the chemical composition of the TaC phase with temperature (according to Thermo-Calc)

tion of the back centred cubic matrix evolves from its crystallization start (1532.75°C) to the end of solidification (1450.74°C), from 36.18Cr-0.03C-3.39Ta to 35.41Cr-0.09C-0.72Ta (wt.%). The chromium content variation of the BCC matrix is not significant between the end of solidification and the beginning of sigma phase appearance. Indeed, between 1450 and 800°C (more precisely 1450.74°C and 795.96°C) its Cr content remains close to 35.5wt.%. In contrast, at the same time, its C and Ta weight contents decrease from 0.09C and 0.72Ta to 0C and 0.01Ta (wt.%).

Thereafter, the change of half BCC matrix in FeCr sigma phase provokes great variations of the chromium and of iron content: at 500°C the BCC matrix ought to become poorer in chromium (17.67wt.%) and then richer in iron (82.33wt.%), while C and Ta may have totally left the BCC matrix (both 0 wt.%).

From their appearance (826.11°C) down to 500°C the chemical composition of the $Cr_{23}C_6$ carbides also varies (Figure 5)., from 15.94Fe-78.43Cr-5.62C to 6.67Fe-87.67Cr-5.66C (wt.%) while tantalum never exists in this carbide whatever the temperature. Thus, iron which partly substituted chromium in the carbide at high temperature, progressively leaves this phase when temperature decreases.

To finish with the results of thermodynamic calculations one can remark that the discard to 50wt.%-50wt.% (but not exactly 50at.%-50at.% of course) of

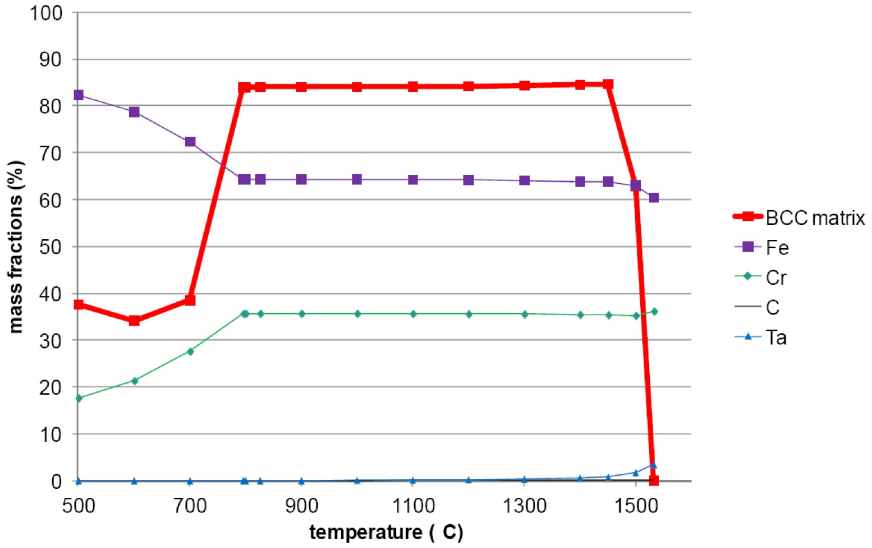

Figure 4 : Evolution of the chemical composition of the BCC matrix phase with temperature (according to Thermo-Calc)

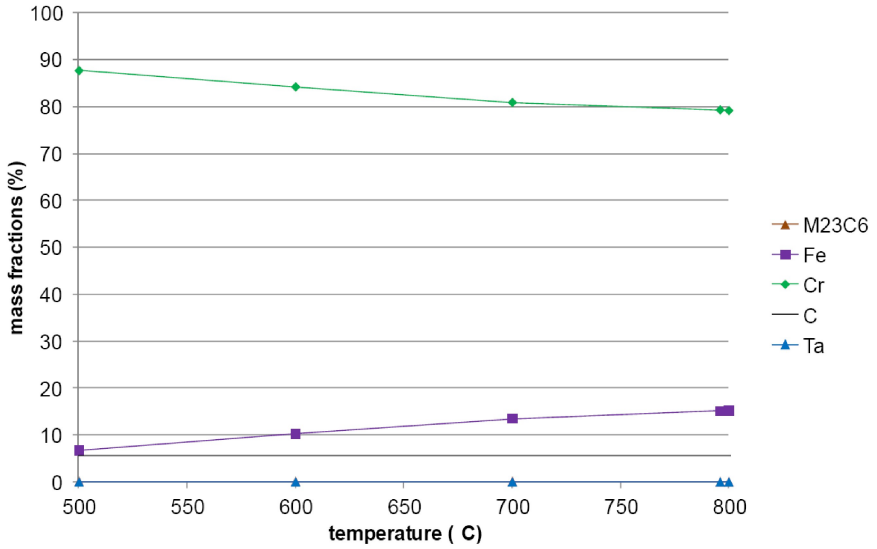

Figure 5A : Evolution of the chemical composition of the $M_{23}C_6$ phase with temperature (according to Thermo-Calc)

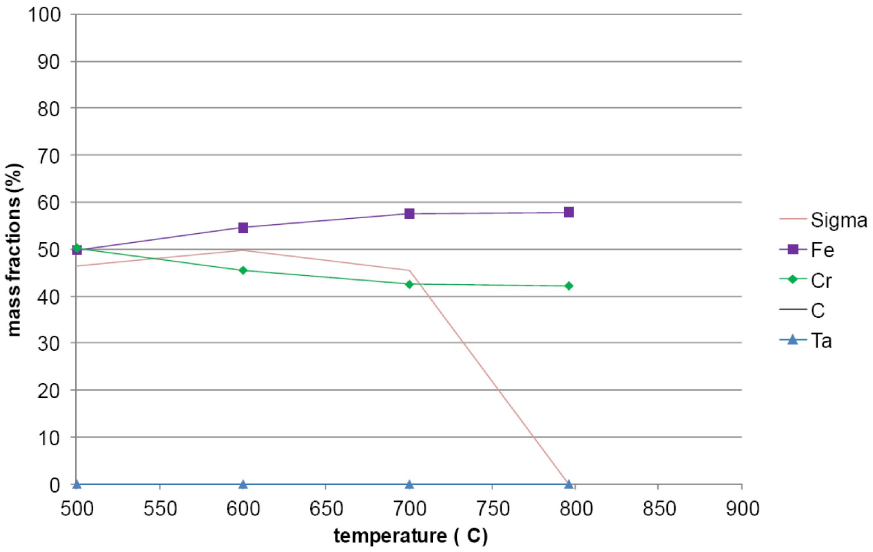

Figure 5B : Evolution of the chemical composition of the sigma phase with temperature (according to Thermo-Calc)

the chemical composition of the FeCr sigma phase existing at its appearance at about 800°C (795.96°C) tends to disappear by evolving from 57.85Fe-42.15Cr to 49.77Fe-50.23Cr (wt.%) at 500°C.

Thus, even if these calculations performed by supposing a thermodynamic equilibrium constantly respected during solidification and solid state cooling do not claim representing with fidelity what should really happen for the microstructure of the alloy, the preceding graphs show that some segregation phenomena may occur during solidification as well as phase transformations during solid state cooling. The most important result is that the almost single carbide expected in the as-cast microstructure is TaC.

The obtained as-cast microstructure

A micrograph illustrating the microstructure of the Fe-30Cr-1C-15Ta alloy is presented in Figure 6. One can immediately see that it does not correspond to what was previously predicted by Thermo-Calc: the TaC phase is not the single carbide present since there are also a lot of chromium carbides. Both carbides form an eutectic with the matrix, and in some locations, they can be mixed together (TaC, chromium carbide and matrix). This discard between the calculated results and the microstructure really obtained can be explained by the real chemical composition of the alloy – assessed by EDS measurement performed with the SEM – which is much poorer in tantalum than targeted. Indeed almost only a part of the whole tantalum added is really in the alloy. A possible reason for that is the loss of a part of the tantalum carbides early formed at the beginning of solidification which have maybe migrated toward the periphery of the mushy alloy before that the dendrites of matrix grow sufficiently to obstruct this TaC phase move. As demonstrated by the previously performed thermodynamic calculations (Figure 1) the TaC phase may be the single solid phase during the loss of the first 500°C during the pro-eutectic part of solidification. Such isolated particles may have moved towards the outer surface of the semi-solid ingot because of the electromagnetic stirring induced by the high frequency induction heating. This possibly changed the thermochemical equilibrium in the core of the ingot with, as possible consequence, the local precipitation of not only eutectic tantalum carbides but also eutectic chromium carbides at the end of solidification. Another possibility is the not total melting of some parts of pure tantalum. Thus the studied alloy the microstructure of which is illustrated in Figure 6 and which was tested in high temperature oxidation is not really Fe-30Cr-1C-3Ta (wt.%) but a Fe-34Cr-1C-6Ta (wt.%) alloy as identified by EDS. The increase in Cr content and in Fe content is to be attributed to the loss of tantalum which induced locally an increase of the contents of all the other elements.

Several pinpoint EDS measurements were performed in the microstructure to help identifying phases (type of carbide) or to specify their own chemical composition (e.g. Cr and Ta in matrix). Such results are

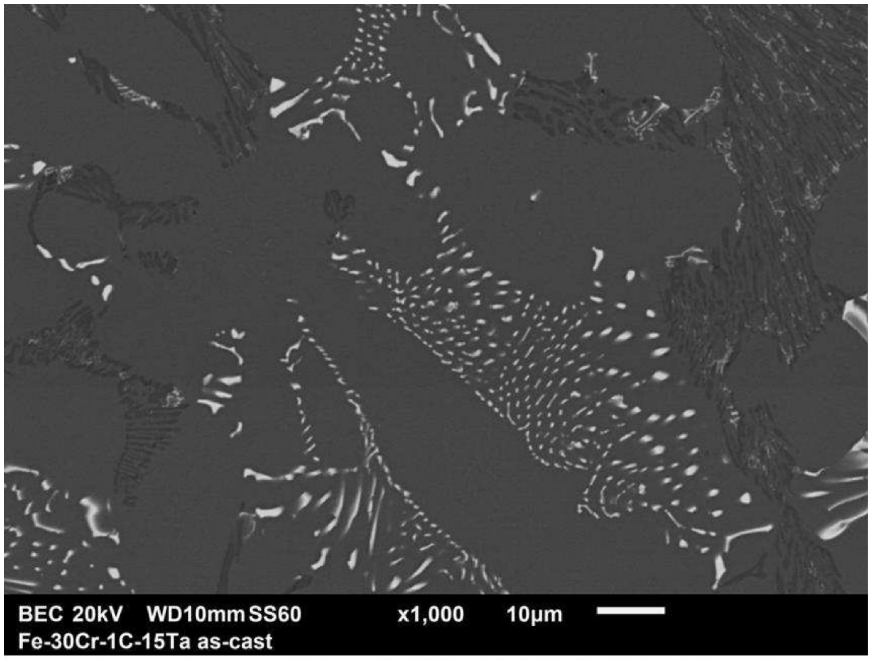

Figure 6 : The as-cast microstructure of the Fe-30Cr-1C-15Ta and the obtained general chemical composition of the alloy (SEM/BSE micrograph; EDS measurement)

given in Figure 7, in which it can be seen that the darkest particles – rich in chromium – are effectively probably chromium carbides (despite carbon cannot be detected and its content measured by this technique) while the white particles are rich in tantalum and thus are probably TaC carbides. The matrix also contains a great part of chromium but its Ta content is rather low.

Three Vickers indentations were realized under a load of 30kg in the metallographic as-cast sample. The obtained values are presented in TABLE 1 which shows that the average hardness of the alloy is not very high, significantly lower than the cobalt alloy studied in the first part of this work (about 435 Hv_{30kg}), and even slightly lower than the nickel alloy of the second part

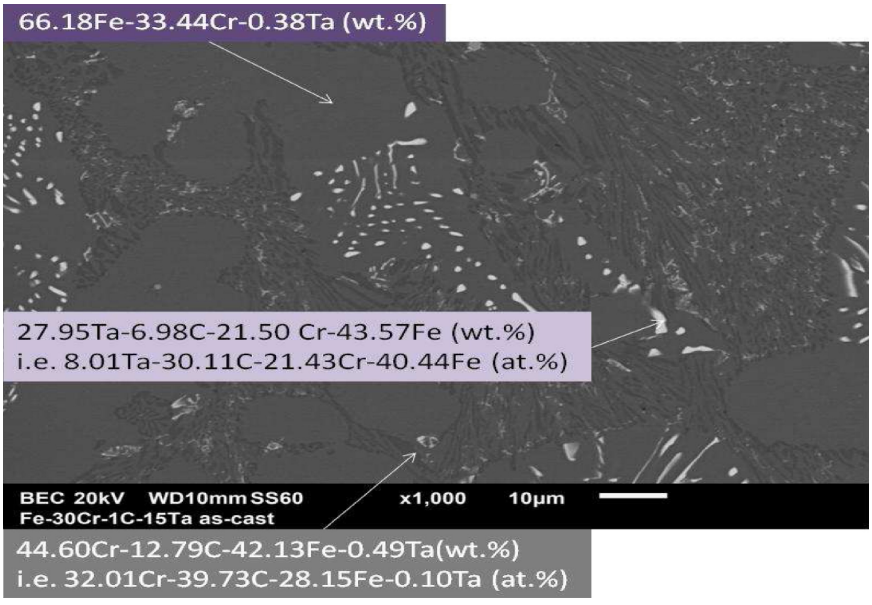

Figure 7 : Some results of matrix chemical composition and of particles identification (SEM/BSE micrograph; EDS measurement)

Full Paper

TABLE 1 : Results of Vickers indentations on the as-cast alloy (load : 30 kg)

Individual values	Average hardness	Standard deviation
269-263-266	266	3

(about 293 Hv_{30kg}).

Behaviour in high temperature oxidation

The surface state of the sample which was exposed in the air of the laboratory during 46 hours at 1150°C (tubular furnace) was observed using the SEM. It is illustrated in Figure 8 by a SEM/BSE micrograph.

An external oxide was here too covering the alloy surface during the high temperature exposure, but this scale was again partly lost during the cooling. However some scale parts still remained on surface and allowed further characterization. In this iron alloy too, disappearance of carbides occurred near the surface while internal oxidation is visible in the subsurface, with the existence of a population of pale oxides in the most external part of the carbide-free zone. One can notice that the average depth of this carbide-free zone, is of about 70µm as for the nickel alloy, and thus twice the one observed for the cobalt alloy. Deeper one can see a curious phenomenon: there is a 200µm-thick part of alloy, starting at a deep of about 100µm under the extreme surface of the alloy, which is especially rich in dark particles.

EDS pinpoint measurements were realized on the different types of oxides (Figure 9), as well as on some of the previously cited dark particles, the results being presented in TABLE 2. The dark oxide formed all around the sample (and which was partly lost during the cooling and by spallation) is chromia. The white oxides present as isolated particles in the most external part of the carbide-free zone are $CrTaO_4$. The dark particles, obviously rich in carbon and in chromium, are probably chromium carbides, much coarser and/or richer in carbon than the eutectic chromium carbides still existing in the not oxidation-affected part of the bulk. Such phenomenon, already encountered in other carbides-containing chromium-rich alloys, may be attributed to an inward diffusion of the carbon atoms liberated from the disappearing carbides of the growing carbide-free zone.

A series of EDS pinpoints measurements was realized in the sub-surface at an increasing depth from the oxide/alloy interface (locations visible in Figure 9). The results, which are displayed in TABLE 3, show that the chromium-depleted zone is not very impoverished in this element since Cr contents as high as 27 wt.% exist very close to the extreme surface. It is consequently

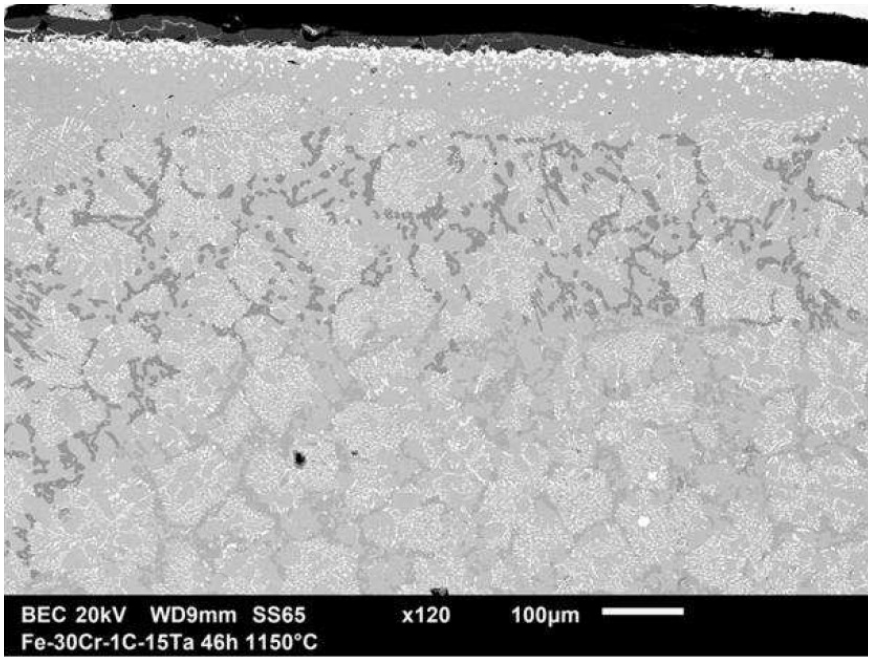

Figure 8 : General aspect of the external surface of the sample after exposure to laboratory air at 1150°C during 46 hours (SEM/BSE micrograph)

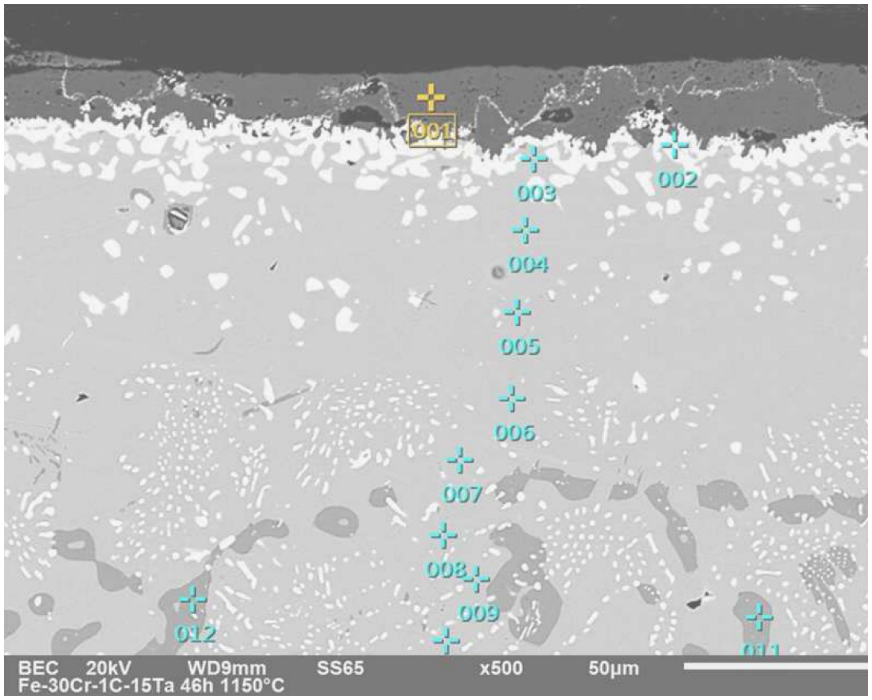

Figure 9 : Locations of the EDS measurements (SEM/BSE micrograph)

TABLE 2 : Chemical composition of the two types of oxides formed on surface and in the subsurface, and of the dark carbides existing deeper than the carbide-free zone; locations numbered according to Figure 9

Oxides' compositions in at.% (and wt.%)	O or C	Cr	Ta	Fe
001	65.21 at.% O	34.60 at.%	0.04 at.%	0.15 at.%
($\rightarrow Cr_2O_3$)	(36.51 wt.%)	(62.95wt.%)	(0.24 wt.%)	(0.30 wt.%)
002	57.86 at.% O	19.31 at.%	19.03 at.%	3.81at.%
($\rightarrow CrTaO_4$)	(16.57 wt.%)	(17.98 wt.%)	(61.64 wt.%)	(3.81 wt.%)
011	31.49 at.% C	62.27 at.%	0.52 at.%	5.71 at.%
	(9.39 wt.%)	(80.35 wt.%)	(2.34 wt.%)	(7.91 wt.%)
012	26.91 at.% C	66.34 at.%	0.72 at.%	6.04 at.%
	(7.62 wt.%)	(81.36 wt.%)	(3.06 wt.%)	(7.95 wt.%)

difficult to measure the Cr-depleted depth with accuracy. With such still high chromium contents close to the oxide/alloy interface one can guess that the chromia-forming behaviour of the alloy, proved by the presence of a (probably) continuous Cr_2O_3 scale protecting the alloy during the exposure at high temperature, will be maintained several supplementary tens and even hundreds hours.

General commentaries

This alloy cannot be really compared to the cobalt and nickel alloys studied in the two first parts of this study because of a Ta content too much different (only 5.7wt.% against slightly less than 15 wt.%). But this discard shows that the initial composition of the present alloy causes a problem for its elaboration by high frequency induction melting because of the too wide range of temperatures across which only TaC exists as solid phase. This led to a microstructure composed of as many chromium carbides as tantalum carbides and not of ex-

TABLE 3 : Evolution of the local chemical composition with the depth from extreme surface (EDS pinpoint analysis); locations numbered according to Figure 9

003	004	005	006	007	008	009	010	Element (wt.%)
26.77	27.54	28.10	28.61	27.38	27.31	27.27	28.28	Cr
0.33	0.43	0.14	0.23	0.16	0.29	0.06	0.10	Ta
72.90	72.02	7177	71.16	72.46	72.40	72.67	71.61	Fe

clusively or mainly TaC. However, the study of the part – obviously homogeneous – impoverished in tantalum (and maybe also in carbon) is still interesting that this showed that an alloy with such composition, is effectively not really hard, but resists more than correctly to high temperature oxidation. This can be interest for some high temperature applications needing high mechanical properties at elevated temperatures other than wear resistance (creep for example).

CONCLUSIONS

The studied alloy probably suffered from some of the characteristics of the used elaboration mode which generated an electromagnetic stirring causing an outward move of the pro-eutectic TaC carbides. The alloy consequently impoverished in tantalum does not present here a microstructure with only TaC carbides, then with high carbides fraction, and consequently a high hardness. However the carbides still present are probably enough for allowing a good creep resistance at high temperature (maybe weakened in another field by the not compact BCC crystalline network of the chromium-rich iron-based matrix), but surely a high resistance against high temperature oxidation as demonstrated here.

REFERENCES

[1] K.Kshitake, H.Era, F.Otsubo; Scr.Metall.Mater., **24**, 1269 **(1990)**.
[2] A.Litwinchick, F.X.Kayser, H.H.Baker, A.Henkin; J.Mater.Sci., **11**, 1200 **(1976)**.
[3] H.E.N.Stone; J.Mater.Sci., **14**, 2787 **(1979)**.
[4] B.V.Cockeram; Metall.Trans.A, **33**, 3403 **(2002)**.
[5] E.F.Ryntz, H.L.Arnson; Modern Casting, **66**, 53 **(1976)**.
[6] P.Berthod; Materials Science and Technology, **25**, 1003 **(2009)**.
[7] P.Berthod, E.Souaillat, O.Hestin, Th.Schweitzer; Materials Science: An Indian Journal, **8(6)**, 234 **(2012)**.
[8] L.Corona, P.Berthod; Materials Science: An Indian Journal, submitted.
[9] L.Corona, P.Berthod; Materials Science: An Indian Journal, submitted.
[10] Thermo-Calc version N: Foundation for Computational Thermodynamics Stockholm, Sweden, Copyright, **(1993,2000)**.
[11] SGTE: Scientific Group Thermodata Europe database, update, http://www.SGTE.org, **(1992)**.
[12] P.Gustafson; Scan.J.Metall., **14**, 259 **(1985)**.
[13] J.O.Anderson, B.Sundman; Calphad, **11**, 83 **(1987)**.
[14] J.O.Anderson; Calphad, **11**, 271 **(1987)**.
[15] J.O.Anderson; Met.Trans.A, **19A**, 627 **(1988)**.
[16] K.Frisk, A.Fernadez Jguillermet; J.Alloys Compnds., **238**, 167 **(1996)**.
[17] N.Dupin, I.Ansara; J.Phase Equilibria, **14**, 451 **(1993)**.